Proceedings of ICFA Mini-Workshop on Tracking for Collimation in Particle Accelerators, CERN, Geneva, Switzerland, 30 October 2015, CERN Yellow Reports: Conference Proceedings, Vol. 2/2018, CERN-2018-011-CP (CERN, Geneva, 2018)

First simulations of collimation cleaning performance for the FCC-hh

M. Fiascaris[*], *R. Bruce, S.Redaelli*
CERN, Geneva, Switzerland

Abstract
In the context of the Future Circular Collider Study (FCC), the FCC-hh is designed to collide protons at the unprecedented energy of 50 TeV and a total stored energy of 8500 MJ per beam. This puts extremely tight requirements on the collimation system to efficiently intercept unavoidable beam losses. In this paper the first FCC-hh cleaning simulations at injection and collision energy are presented. The collimation layout includes betatron and momentum cleaning, as well as dump protection collimators and collimators in the experimental insertions for protection of the inner triplets. The simulation setup and the developments that were necessary to achieve these first simulation results are described. The performance of the system is then assessed through the analysis of complete loss maps for a perfect machine.

Keywords
FCC-hh; collimation; tracking simulations.

1 Introduction

The hadron-hadron option of the Future Circular Collider study, FCC-hh [1], is designed to provide pp collisions at a centre of mass energy of 100 TeV. For a nominal beam intensity of 10^{15} protons, the total stored energy per beam will be about 8500 MJ, a factor of 20 above that of the LHC. The high energies and intensities required at the FCC-hh pose daunting challenges on the control of beam losses. Its beams are highly destructive: uncontrolled losses of even just a small fraction of the beam can cause a magnet to quench or damage to accelerator components.

A collimation system is needed to intercept and safely dispose of unavoidable beam losses. Its main functionalities are: efficient cleaning of the beam halo ensuring an operation safely below quench limits at injection and top energy, passive protection of the machine aperture against abnormal losses and minimisation of the halo-induced experimental backgrounds. In this paper, only beam halo cleaning is considered since this is expected to be the driving constraint for the FCC-hh collimation system. At the LHC this is achieved through a multi-stage cleaning [2] with two dedicated insertions for betatron and momentum collimation. Given the excellent performance of the LHC collimation system, validated up to energies of 6.5 TeV and stored beam energy of about 250 MJ, the first conceptual solution for the FCC-hh collimation is a scaled-up system derived from the present LHC. This conservative, but solid approach allow us to evaluate the performance that we can achieve with the current state-of-the-art and to start a mechanical design based on a first assessment of powerloads. Further improvements and technological developments will be considered at a later stage.

In this paper, we present the first simulation setup developed to study the cleaning performance of the FCC-hh collimation system. After a description of the system layout and optics, the parameters used to define the system cleaning performance are described. The tracking tools used to achieve the simulations are then presented, with emphasis on the developments needed to adapt the existing tools to the FCC-hh case. Finally, the results of detailed particle tracking simulations are shown and the performance of the system at injection and collision energy is assessed through the analysis of proton loss maps.

[*]maria.fiascaris@cern.ch

https://doi.org/10.23732/CYRCP-2018-002.171.

2 Baseline for the FCC-hh collimation system

In the baseline FCC-hh layout [3], described in Table 1 and shown in Fig. 1 [4], momentum and betatron cleaning are performed in two separate insertions. The so called Extended Straight Section D (ESS-D) is dedicated to the beam extraction followed by betatron collimation on one beam (B1), while momentum collimation is performed on the counter-rotating beam (B2). Similarly, in the ESS-J momentum cleaning is performed on B1 and extraction followed by betatron collimation on B2. In the rest of this paper we will consider B1 only, therefore it is assumed that betatron cleaning is implemented in ESS-D and momentum cleaning in ESS-J.

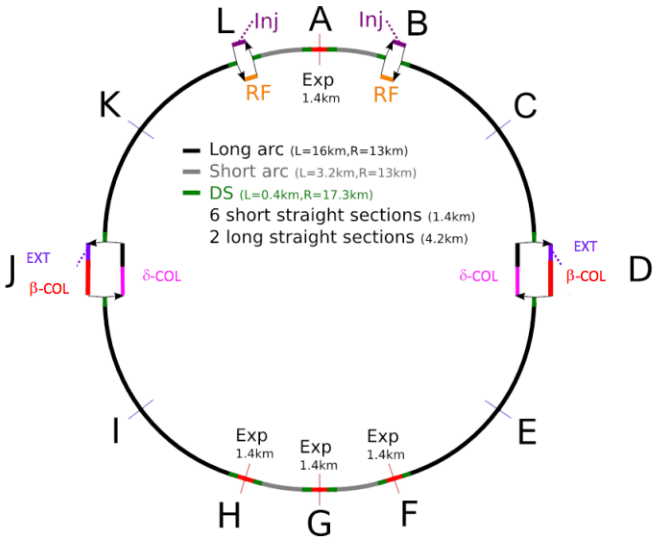

Fig. 1: Schematic layout of the FCC-hh with the configuration of the extraction, momentum and betatron collimation in the extended straight sections D and J.

Table 1: Parameters of the FCC-hh ring. The lattice v7 [5] was used. The scale factor k for the cleaning insertions refers to the factor used to scale the betatron functions from the LHC to the FCC-hh. For the interaction region, the ultimate $\beta^\star$ value at 50 TeV energy is indicated.

Parameter	**Value**
Circumference	100.171 km
Betatron cleaning insertion:	
Scale factor k	5
Length	2.7 km
Momentum cleaning insertion:	
Scale factor k	2.7
Length	1.4 km
Interaction regions:	
$\beta^\star$	0.3 m
$L^\star$	45 m
Normalised emittance	2.2 μm

The optics functions for betatron cleaning are shown in Fig. 2 (left). They are similar to the ones used in LHC, except that they are scaled up by a factor $k = 5$, resulting in an insertion length of 2.7 km. The scaling factor was chosen to achieve collimator gaps that are similar to the LHC ones both in units of the beam standard deviation σ and mm, in order to avoid excessive impedance and to guarantee

mechanical stability while keeping the σ-setting small enough to protect the aperture. The number of collimators and their phase advances are the same as in the LHC and were optimised for three-stage cleaning [6]. Primary collimators (TCP), closest to the beam, intercept primary proton losses and give rise to a secondary halo that is intercepted by secondary collimators (TCS). Active absorbers (TCLA), placed outside TCS, catch showers from upstream collimators.

A similar three stage cleaning is installed in ESS-J for momentum collimation, with the difference that the horizontal dispersion in ESS-J is much higher than in ESS-D (see Fig. 2 right). The dispersion functions of the momentum cleaning insertion are the same as at the LHC. The betatron functions are scaled with a factor $k = \sqrt{50/7} = 2.7$, derived from the ratio of the centre-of-mass energies of the FCC-hh to the LHC. This scaling factor is smaller than that used for the betatron cleaning insertion allowing to shorten the length to 1.4 km. Constraints from impedance and mechanical stability are in fact less tight in the momentum cleaning insertion because primary collimators for momentum cleaning can be kept more opened in σ than the ones for betatron cleaning. The momentum cleaning system is designed to capture losses only in the horizontal plane, while the betatron cleaning system ensures coverage in the whole transverse space.

In addition, tertiary collimators (TCT) are installed in the low-beta insertions, about 220 m upstream the interaction point, to provide local protection of the inner triplets. At the beam extraction, a dump protection collimator (TCDQ) is installed as a protection against miskicked beams in the case of extraction failures.

The same collimator jaw materials and lengths as at the LHC are assumed. These are summarised in Table 3. It is planned to modify the collimator materials in the future, based on the outcome of new material studies that are ongoing in the context of the HL-LHC upgrade [7]. Further improvements of the system, such as addition of more collimators and optimisation of phase advances are also foreseen.

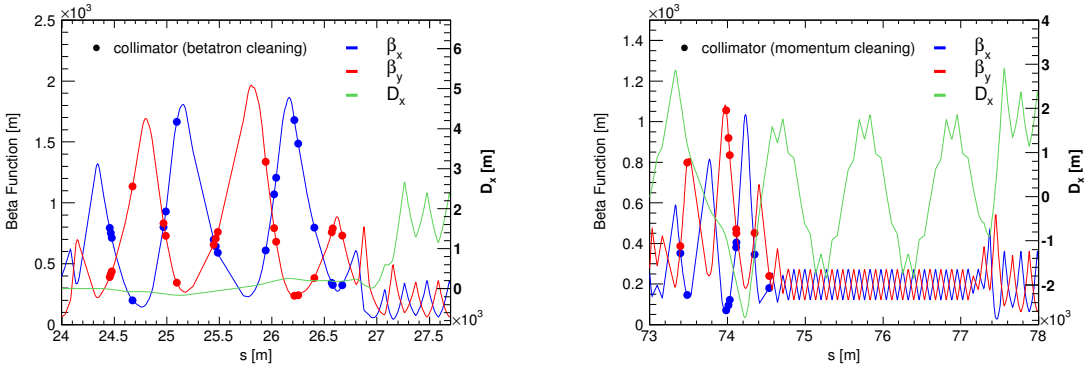

Fig. 2: Optical functions for the betatron (left) and momentum (right) cleaning insertions. The markers show the location of collimators.

3 Simulation of collimation performance

3.1 Cleaning performance

The performance of the collimation system is described by the cleaning inefficiency η_c, defined as the ratio of surviving protons above a given amplitude A_0 to the number of protons absorbed by the collimation system (N_{abs}):

$$\eta_c(A_0) = \frac{N_p(A > A_0)}{N_{\mathrm{abs}}}. \quad (1)$$

Losses are distributed longitudinally over some dilution length. It is therefore useful to define a local cleaning inefficiency $\tilde{\eta}_c$ which is a function of the longitudinal coordinate s and has units of 1/m. Detailed

tracking simulations are used to predict $\tilde{\eta}_c$ along the accelerator with a resolution determined by the bin size Δs:

$$\tilde{\eta}_c(s) = \frac{1}{\Delta s} \cdot \frac{N_{\text{loss}}(s \to s + \Delta s)}{N_{\text{abs}}}, \tag{2}$$

where $N_{\text{loss}}(s \to s + \Delta s)$ is the number of particles lost in the aperture between position s and $s + \Delta s$.

The key parameters that determine the target performance of a collimation system are the beam intensity N_{tot}, the minimum allowed beam lifetime τ_b and the quench level R_q. These are related to collimation cleaning inefficiency by the following equation, which describes the condition for operating the machine ensuring that losses in the cold magnets remain below the quench limit:

$$\frac{N_{tot}}{\tau_b} \times \tilde{\eta}_c < R_q. \tag{3}$$

The relevant parameters for the FCC-hh are summarised in Table 2. The minimum allowed beam lifetimes at injection and top energy are assumed to be the same as at the LHC. Quench limits for the FCC-hh are not yet available. However using simple scaling assumptions from the LHC value of $R_q = 7.6 \times 10^6$ p/m/s at 7 TeV [8], the quench level for the FCC-hh at 50 TeV was estimated at $R_q = 0.5 \times 10^6$ p/m/s [9]. Substituting this values into Eqn. 3 and assuming $\tau_b = 0.2$ h, the required cleaning inefficiency at 50 TeV is calculated to be 3×10^{-7} m^{-1}. In the absence of more accurate estimates, this target value will be taken as a benchmark to asses to the performance of the system in Sec. 5.2. Given that the performance requirements are most stringent at collision energy, a solution for 50 TeV energy also fulfills the requirements at injection energy.

Table 2: Beam parameters and assumptions on the minimum allowed beam lifetime for the FCC-hh at injection and collision energy.

FCC-hh	**Injection**	**Collision**
Beam energy [TeV]	3.3	50
Beam intensity (N_{tot})	$1 \cdot 10^{15}$	$1 \cdot 10^{15}$
Stored energy [MJ]	560	8500
Assumed minimum beam lifetime (τ_b)	0.1 h	0.2 h
Power load ($t = \tau_b$) [MW]	1.6	11.8

3.2 Simulation tools for FCC-hh cleaning studies

The cleaning performance of the system was assessed with simulations performed with SixTrack [11–15], a six-dimensional simplectic tracking code. When a particles hits a collimator, a Monte Carlo scattering routine simulates the particle-matter interactions, including Multiple Coulomb scattering, Rutherford scattering, ionisation, as well as point-like interactions such as nuclear elastic, inelastic and single diffractive interactions. The cross-sections of the scattering routine were recently updated taking into account experimental data from the LHC [17]. Since the process of interest is the impact of a high energetic proton on a fixed target (the collimator jaw), the centre-of-mass energy under study is $\sqrt{s} = 306$ GeV for a 50 TeV beam, only 2.7 times higher than at the LHC collision energy. It is therefore expected that the extrapolation to the FCC-hh energies does not significantly affect the reliability of the simulations. In order to validate this assumption, different tracking codes were compared and the level of agreement was found to be satisfactory [18, 19].

The tracking code records the trajectories of halo particles along the accelerators, which are then used as input to an aperture programme [20] to predict the longitudinal distribution of losses, producing so called loss maps. This aperture programme interpolates the saved trajectories and finds the location

where a given trajectory intercepts the machine aperture with a resolution of 10 cm. For the FCC ring, this effectively implies checking the transverse position of each particles for 1 million points.

The SixTrack code and aperture programme were developed for LHC studies. Several developments were needed to achieve the cleaning performance simulations presented in this paper. The existing code had to be adapted to account for the longer ring and the large number of elements in the accelerator structure. Furthermore a first aperture module for the FCC-hh had to be defined [21]. The geometrical aperture of the arc was given by the beam screen, assumed to be of rect-ellipse shape and dimensions 2×15 mm (width) and 2×13.2 mm (height). In the collimation insertion and matching sections, the same mechanical aperture as in the LHC was assumed. The mechanical aperture in the experimental insertion was designed as described in [22].

A major challenge for the FCC-hh simulations was the computing performance. The size of the ring resulted not only in much higher CPU usage, but also in very large size of the intermediate files containing the particle trajectories used for the aperture checks. As a result, the simulations had to be split into a large number of small size jobs, each job tracking about 2 thousands particles. In order to maximize the efficiency of the simulations, the initial particle distribution was chosen such that the majority of particles impacted the primary collimator at the first turn. Details of the simulation parameters and the initial distributions are described in Section 5.

4 Baseline collimator settings

Collimator settings have to be defined in a way that ensures protection of the minimum machine aperture with sufficient margin. Furthermore, a strict hierarchy between collimator families must be respected for optimal cleaning performance and machine protection.

By design at collision energy the aperture limitation typically lies in or close to the inner triplet, since at this location the available aperture is reduced by the large beta functions required to achieve small beam sizes at the interaction points and by the crossing and separation schemes. This constrains the opening of the tertiary collimators (TCT). In the present LHC system, TCTs are not robust and have to be placed outside protection devices, such as the TCDQ, which in turn should be at larger aperture than TCPs and TCSs. For FCC-hh, we define settings in a similar way to minimise the risk of major losses close to the experiments. At injection energy the aperture bottleneck is instead in the arc, which has to be protected by the betatron and momentum cleaning systems, while the TCTs can be more open.

In Table 3 we present the baseline collimator settings for the FCC-hh at injection and collision energy that provide a minimum protected aperture of 15.5 σ. These settings correspond to the HL-LHC baseline settings [24] scaled to the FCC-hh normalised emittance of 2.2 μm and result in collimator gaps (in mm) that are comparable to the LHC ones.

Detailed aperture studies that take into account optical and mechanical tolerances will be necessary to validate and, if necessary update, the settings at injection and collision energy. In the meanwhile, this first baseline for collimator settings represent a realistic scenario and allows for a first evaluation of the system performance.

5 Tracking simulations

For the simulations presented in this paper, the initial particle distribution was a direct halo [15] at 7.2 σ and a thickness $\delta\sigma = 0.06$ in the horizontal plane, a normal distribution cut at 3 σ in the vertical plane and no energy errors. The average impact parameter b on the TCP was about 16 μm and 4 μm at injection and collision energy, respectively. The effect of the assumed initial distribution was assessed by varying the impact parameter b on the primary collimator between $1\mu\mathrm{m}$ and $12\mu\mathrm{m}$. The cleaning inefficiency was found to change by about 20% between the extreme values of b.

Large statistics is needed to reach a precision level for loss spikes which is below the assumed

Table 3: Baseline collimator settings at injection (3.3 TeV) and collision (50 TeV) energy, expressed in units of σ for a normalised emittance of 2.2 μm.

Description	Name	Length [m]	Material	Settings [σ]	
				Injection (3.3 TeV)	Collision (50 TeV)
Betatron cleaning	TCP	0.6	C	7.2	7.2
	TCS	1.0	C	9.7	9.7
	TCLA	1.0	W	12.0	12.0
Momentum cleaning	TCP	0.6	C	11.0	21.4
	TCS	1.0	C	12.6	25.2
	TCLA	1.0	W	16.0	27.7
Extraction Tertiaries	TCDQ	9.0	C	11.4	11.4
	TCT	1.0	W	30	13.7

quench levels. Therefore, for the simulations presented here, 8.9 million particles were tracked for 200 turns for the case of a perfect machine and using collimator settings from Table 3.

Figure 3 shows the distribution of inelastic impacts (including nuclear inelastic scattering and single diffractive events) on the three primary collimators of the betatron cleaning insertion ESS-D. This is an example of distributions that can be used as input for further studies of detailed energy deposition.

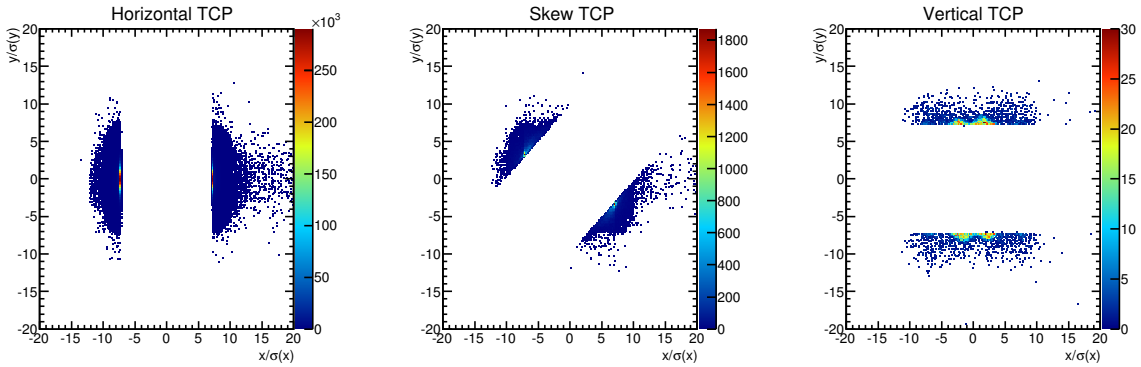

Fig. 3: Distribution of inelastic impacts on the three primary collimators of the betatron cleaning insertion ESS-D.

5.1 Cleaning inefficiency

A first assessment of the collimation system performance can be made studying the cleaning inefficiency η_c, as explained in Sec. 3. η_c has the advantage of being independent of the longitudinal coordinate s and can be studied without an aperture model. Eqn. 1 defines η_c as a function of the radial amplitude A_0. Similarly, to study the off-momentum population, we can define a cleaning inefficiency as a function of the relative momentum deviation $\delta p/p$, by substituting into Eqn. 1 the amplitude A with $\delta p/p$. The cleaning inefficiency of the system is shown in Figure 4 at both injection and collision energy. At an aperture of 15.5 σ, corresponding to the minimum protected aperture for the baseline collimator settings, the cleaning inefficiency is below 10^{-4}, while at $\delta p/p = 0.7\%$, corresponding to the momentum acceptance of the arc, the cleaning inefficiency is below 10^{-6}.

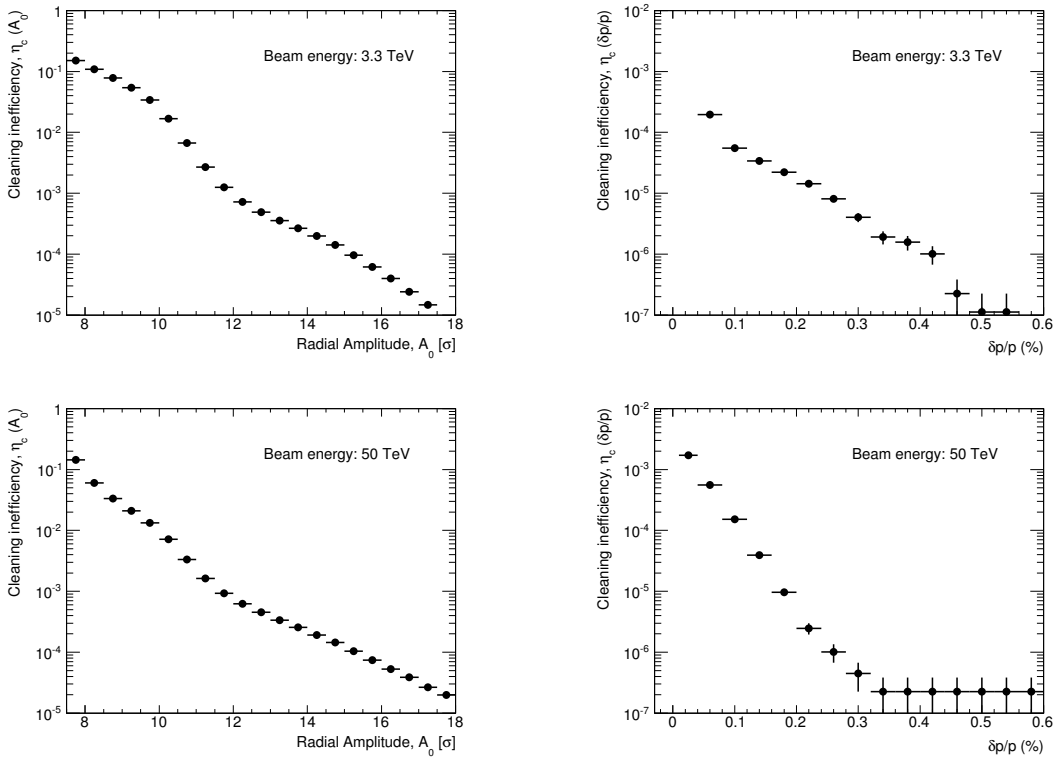

Fig. 4: Cleaning inefficiency as a function of radial amplitude A_0 (left) [23] and momentum off-set $\delta p/p$ (right) at injection (top) and collision (bottom) energy. The horizontal error bars represent the bin width, while the vertical ones are the statistical errors on the efficiency and are calculated using the binomial approach [16] as $\sqrt{\eta_c(1-\eta_c)/N_{abs}}$, where η_c and N_{abs} are defined in Eqn. 1.

5.2 Loss maps for a perfect machine

Loss maps allow to study the local cleaning inefficiency $\tilde{\eta}_c$, that is how particles escaping the collimation system are lost longitudinally around the ring. Horizontal loss maps are shown in Fig. 5 and Fig. 6 [23] for injection and collision energy, respectively, for a resolution of 10 cm in s. A zoom is shown in locations with large losses: the betatron and the momentum cleaning insertions and one of the two interaction points. It should be noticed that the loss maps shown in this paper consider betatron losses only and the only off-momentum component arises from interactions with the collimators. As a result losses in the betatron cleaning insertion are much larger than in the momentum cleaning insertion. Complementary studies of off-momentum losses are ongoing and are not treated here.

The most significant cold losses occur in the dispersion suppressor (DS) downstream of the cleaning insertions, where two clusters of losses are observed in correspondence to local peaks in the dispersion function. The peak cleaning inefficiency is reached in the second cluster of ESS-D with a value of $(1.1 \pm 0.4) \times 10^{-5}$ m^{-1} and $(3.7 \pm 0.6) \times 10^{-5}$ m^{-1}, at injection and collision energy, respectively. At collision energy, this value is about two orders of magnitude above the assumed quench level of 3×10^{-7}m^{-1}. These losses are due to particles from single diffractive interactions at the primary collimators.

Other important losses occur around the interaction point (IP) in correspondence of aperture restrictions at the location of the recombination dipoles. At injection energy, these losses are higher than those in the DS regions downstream of ESS-D. If the magnet aperture cannot be increased, these losses can be cured by carefully positioning tertiary collimators for local protection of the dipole magnets.

At collision energy, losses at the level of 6×10^{-6} are also observed in the dispersion suppression

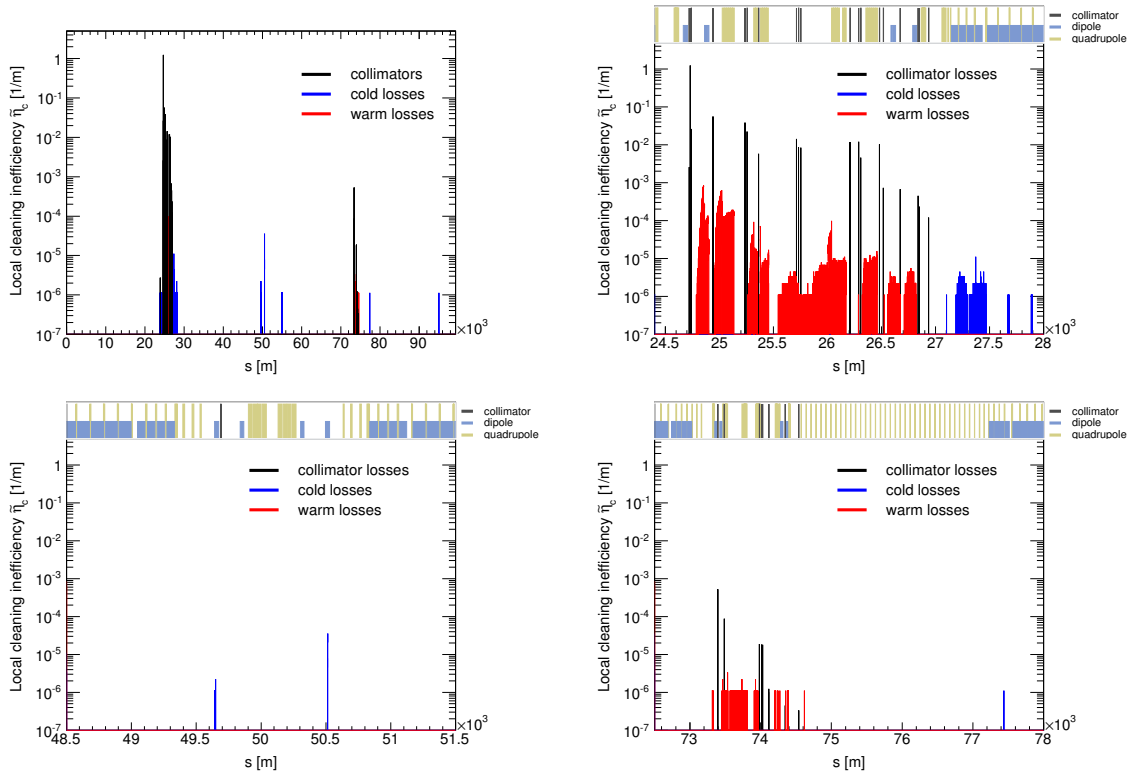

Fig. 5: Horizontal loss map at injection energy of 3.3 TeV for the entire ring (top left), zoom in the betatron cleaning insertion ESS-D (top right), in the interaction point G (bottom left) and in the momentum cleaning insertion ESS-J (bottom right) [23]. The interaction points A and G are located at $s = 0$ and 50×10^3 m respectively, while ESS-D and ESS-J start at about $s = 23 \times 10^3$ and 73×10^3 m respectively.

region after the IP, in correspondence to local peaks in the dispersion function. Such losses are not observed at injection energy: tertiary collimators are in fact retracted and protons are intercepted earlier by the aperture restriction in correspondence of the recombination dipole.

These studies allow to identify the main performance limitation of the system in the losses in the DS after the betatron cleaning insertion. Similar performance limitations are observed at the LHC and have been extensively studied in the context of the HL-LHC upgrade [25]. The LHC solution consists in the installation of new collimators in the DS upstream of the critical locations. This solution intercepts locally beam halos with a significant off-momentum component and has also the advantage to reduce losses in other locations around the ring. At the FCC-hh an analogous solution can be applied and the design of the DS can be optimised to improve the performance of the system with additional local protection collimators. Details of such implementation are being studied for different FCC layout options.

6 Outlook and conclusions

A conceptual design for the FCC-hh collimation system was presented. This first complete baseline comprised betatron and momentum cleaning, with optics scaled from the LHC, dump protection and tertiary collimators. Baseline collimator settings were proposed and the cleaning performance of the system was investigated through detailed tracking simulations. In order to achieve a complete performance evaluation of the FCC-hh collimation system, the simulation tools already used for LHC studies had to be setup for the FCC-hh machine for the first time. The existing tracking code had to be adapted to the FCC case and a first aperture model had to be developed. Achieving detailed loss maps for a ring of the size of

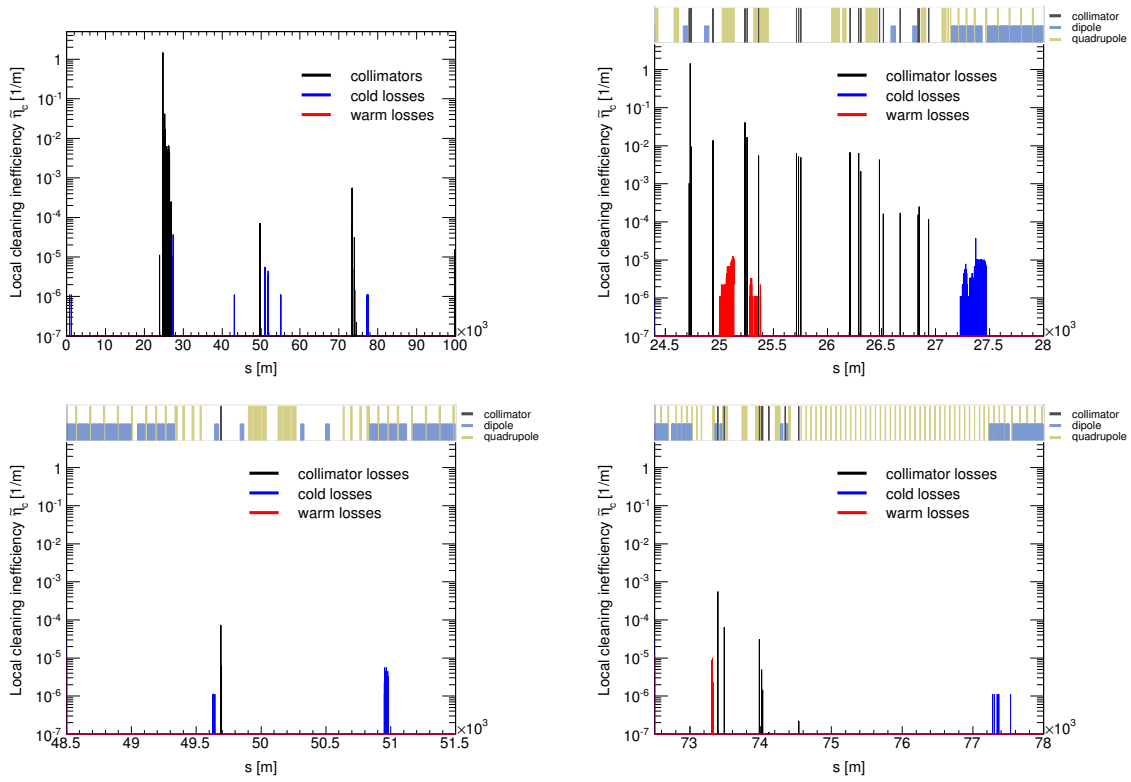

Fig. 6: Horizontal loss map at collision energy of 50 TeV for the entire ring (top left), zoom in the betatron cleaning insertion ESS-D (top right), in the interaction point G (bottom left) and in the momentum cleaning insertion ESS-J (bottom right) [23]. The interaction points A and G are located at $s = 0$ and 50×10^3 m respectively, while ESS-D and ESS-J start at about $s = 23 \times 10^3$ and 73×10^3 m respectively.

the FCC-hh demonstrated to be a challenge in terms of computing performance. This aspect is already being addressed and future FCC studies will profit from the continuous developments on the tracking code [26] aimed to improve its efficiency and capabilities for collimation cleaning.

Similarly to the LHC, the performance limitation of the system was identified to be in the cold losses in the dispersion suppressor downstream of the betatron cleaning insertion. The addition of collimators in the dispersion suppressor and a layout optimisation will be investigated in the future and are expected to provide significant improvements.

Detailed performance estimates can only be assessed once the quench limits of FCC-hh magnets will be known, but this first implementation of a multi-stage system already provides encouraging results. The results of these tracking simulations will provide a first set of input for the collimator hardware design, which should be compatible with the loss scenario of the FCC-hh.

Ackowledgments

References

[1] A. Ball *et al.*, EDMS doc. 134202 (2014).

[2] O. S. Bruening *et al.*, CERN-2004-003-V-1.

[3] A. Chance *et al.*, TUMPW020, Proc. IPAC 2016.

[4] D. Schulte *et al.*, CERN-ACC-2016-0082.

[5] FCC-hh lattice repository, https://gitlab.cern.ch/fcc-optics/FCC-hh-lattice.git.

[6] J. B. Jeanneret, LHC-Project-Report-243 (1998).
[7] E. Quaranta *et al.*, WEPMW031, IPAC 2016.
[8] C. Bracco, "Commissioning Scenarios and Tests for the LHC Collimation System", PhD thesis, EPFL Lausanne, 2008.
[9] D. Schulte, FCC Week 2016, https://indico.cern.ch/event/438866/contributions/1085167.
[10] J. B. Jeanneret, LHC Project Report 1007 (2007).
[11] SixTrack, http://sixtrack.web.cern.ch/SixTrack/.
[12] F. Schmidt, Report No. CERN/SL/94-56-AP (1994).
[13] E. McIntosh, R. De Maria, CERN-ATS-Note-2012-089 TECH.
[14] G. Robert-Demolaize *et al.*, FPAT081, Proc. PAC 2005.
[15] R. Bruce *et al.*, Phys. Rev. ST Accel. Beams 17, 081004 (2014).
[16] T. Ulrich and Z. Xu, arXiv:physics/0701199v2, 2012.
[17] C. Tambasco, CERN-THESIS-2014-014.
[18] M. Fiascaris, Collimation Upgrade Specification Meeting, June 2016, https://indico.cern.ch/event/540629/contributions/2195910/attachments/1289126/1919162/ColUSM73_FlukaCoupling.pdf.
[19] J. Molson *et al.*, EuroCirCol Meeting, ALBA, November 2016, https://indico.cern.ch/event/567230/contributions/2346538/attachments/1367641/2072506/JM-EUROCIRCOL-2016-11-08.pdf.
[20] S. Redaelli *et al.*, LHC Project Workshop, Chamonix XIV, 2005.
[21] M. Fiascaris *et al.*, WEPMW006, Proc. IPAC 2016.
[22] R. Martin *et al.*, TUPTY001, Proc. IPAC 2015.
[23] M. Fiascaris, R. Bruce, S. Redaelli, "First conceptual design of a collimation system for FCC-hh", submitted to Nucl. Instr. Meth. Phys. Res. Sec. A, November 2017.
[24] R. Bruce *et al.*, CERN-ACC-2014-0044.
[25] R. Bruce *et al.*, MOPRO042, Proc. IPAC 2014.
[26] A. Mereghetti *et al.*, "SixTrack for cleaning studies: 2017 updates", Proc. IPAC 2017.